Theoretical Study of the Rates and Mechanism of the Gas-Phase Reaction $H+HN_3 \rightarrow NH_2+N_2$

Takayuki FUENO* and Shin-ya TAKANE
Department of Chemistry, Faculty of Engineering Science, Osaka University, Toyonaka, Osaka 560
(Received February 8, 1993)

Reaction of the hydrogen atom with hydrazoic acid HN_3 in the gas phase has been investigated theoreticallly. Tracing of the reaction path by the SCF procedure based on the 6-31G (d,p) basis functions has shown that the reaction proceeds through an initial rate-determining hydrogen atom addition to HN_3 giving a doublet radical H_2N_3, which is subsequently self-decomposed into NH_2+N_2. The barrier height for the initial addition step calculated by the MRD-CI method employing the [4s2p1d] basis sets is 21 kJ mol^{-1} (with the vibrational zero-point energy correction). The bimolecular rate constants for the overall reaction calculated by the conventional transition state theory combined with appropriate tunneling corrections are found to agree well with the experimental data reported over the temperature range 300 to 500 K.

The bimolecular reaction of the hydrogen atom with hydrazoic acid HN_3 is known to be an unavoidable side reaction in the thermal decomposition of HN_3.[1] It is so much so as the triplet imidogen radicals NH ($^3\Sigma^-$) generated by the primary decomposition of HN_3 tend to be readily "self-recombined" to give N_2+2H. HN_3 as the parent compound is much more susceptible to the attack of H than to NH ($^3\Sigma^-$).

A direct kinetic study[2] of the reaction between H and HN_3 has shown that the product is exclusively NH_2:

$$H + HN_3 \rightarrow NH_2 + N_2 \quad (1)$$

Apparently, reaction (1) is far more advantageous than the abstraction reaction:

$$H + HN_3 \rightarrow H_2 + N_3 \quad (2)$$

The situation can be taken as indicating that the initial step of the H–HN_3 reaction will be an addition reaction

$$H + HN_3 \rightarrow \underset{\mathbf{1}}{\overset{H}{\underset{H}{\rangle}}N\text{–}NN} \quad (3)$$

the doublet adduct thus formed being decomposed subsequently to NH_2+N_2:

$$\mathbf{1} \rightarrow NH_2 + N_2 \quad (4)$$

Admitting that the bimolecular reaction of our concern, i.e., reaction (1), is in reality a two-step reaction comprizing reactions (3) and (4), we are required to answer several questions of importance. They include the following:

1. Can the adduct **1** be a well-definable intermediate?
2. Which of the two successive reactions, (3) and (4), is rate-determining? More specifically, which of the respective transition states will energetically be less stable?
3. Can the characteristics of the net transition state located be compatible with the experimentally determined rate constants[2]?

The present work is aimed at answering all these questions. To this end, we trace reactions (3) and (4) by the SCF/6-31G (d,p) procedure. The stationary points located are then subjected to the multi-reference double-excitation (MRD) configuration-interaction (CI) computations using the [4s2p1d] basis functions. The bimolecular rate constants for the overall reaction (1) are calculated by the conventional transition state theory (TST).[3] Kinetic features and mechanism of the reaction will be discussed in the light of the theoretical results obtained.

Method of Calculations

The reaction paths were traced by the UHF SCF procedure combined with the energy gradient technique. The Gaussian 86 program package[4] was used for this purpose. The basis sets used are the 6-31G(d,p) functions[5] throughout. The validity of the geometries for the transition states located were checked by the vibrational analyses.

All the stationary points involved in the potential energy surface swept were then subjected to the MRD-CI computations. The Table MRD-CI program furnished by Buenker[6,7] was used. The basis sets used for the CI computations were the conventional 6-31G(d,p) functions and the [4s2p]/[2s] functions due to Dunning[8] augmented with one set each of d and p polarization functions. In obtaining the CI energy, we followed the configuration-selection routine, extrapolation technique, and the Langhoff–Davidson perturbation corrections, as has been described in detail in our previous papers.[9—11] The maximal dimension of the present CI computations are ca. 15000 while the total numbers of the symmetry-adapted configurational functions are ca. 800000.

Results

(A) Adduct Radical. The doublet radical H_2N_3 comprizing hydrazoic acid HN_3 and a hydrogen atom can either be an asymmetric entity HHN_3 (**1**) or a symmetric adduct HN_3H (**2**). SCF geometry optimizations of these radicals by use of the 6-31G(d,p) basis sets gave the structures as shown in Fig. 1. The former radical (**1**) has proved to be nonplanar, while the latter (**2**) is planar (C_{2v})symmetric. In terms of the UHF SCF en-

ergies, **1** and **2** are more stable than the binary system $H+HN_3$ by 254 and 184 kJ mol^{-1}, respectively.

By separate computations, it has been confirmed that **1** is state-correlated with $H+HN_3$ ($\tilde{X}^1A'$), whereas **2** with $H+HN_3$ ($\tilde{a}^3A''$). The situation indicates that the addition of the hydrogen atom toward HN_3 in its ground state ($\tilde{X}^1A'$) should take place exclusively on the terminal nitrogen atom bearing the H atom. This, in turn, justifies the presumption that the initial step of the $H-HN_3$ reaction of our present concern will be reaction (3). In what follows, therefore, we will focus our attention on the behavior of the asymmetric radical HHN_3 (**1**).

(B) Potential Energy Profiles. To begin with, the transition state (TS1) of the initial H atom addition reaction (3) was located by the SCF/6-31G(d,p) procedure. The incoming hydrogen atom (H^5) starts to approach the N^1 atomic site from the direction perpendicular to the molecular plane of HN_3. The optimal geometry obtained for TS1 is shown in Fig. 2. The calculated SCF barrier height was 50 kJ mol^{-1}.

The subsequent decomposition process of **1**, reaction (4), was then traced by the SCF procedure in the attempt to locate its transition state (TS2). The SCF saddle point showed up at the N^1–N^2 separation of 1.59 Å. The point was found to lie only 14 kJ mol^{-1} above **1**. TS2 is thus far lower-lying than TS1 and is even more stable than the initial state $H+HN_3$. Clearly, the initial H atom addition step, reaction (3), is rate-determining

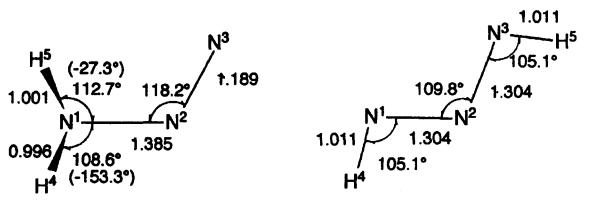

Fig. 1. Optimized geometries of HHN_3 (**1**) and HN_3H (**2**). The bond lengths are given in units of Å. The entries given in parentheses indicate the dihedral angles ϕ (HNNN).

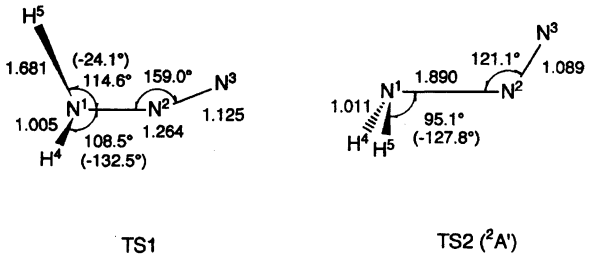

Fig. 2. Optimized geometries of the transition states. The bond lengths are given in units of Å. The entries given in parentheses indicate the dihedral angles ϕ (HNNN). TS1, reaction (3); TS2, reaction (4).

for the overall reaction (1).

All the stationary points mentioned above were subjected to the MRD-CI calculations using the 6-31G(d, p) and Dunning's [4s2p1d] basis functions. The CI energies obtained and the vibrational zero-point corrected data therof (CI+vib), both expressed by taking the initial $H+HN_3$ system as reference, are summarized in Table 1. The UHF SCF energies are also included there for the sake of comparison.

We should mention one thing at this stage. That is, because geometries of the various doublet species treated in this work have all been optimized by the UHF SCF procedure, we feel it most adequate to conduct the geometry optimization for the singlet mother compound HN_3 somehow at a beyond-RHF SCF level. The precaution seems to be particularly appropriate here since the total energy calculated for HN_3 is fairly sensitive to the geometry adopted for it. Under such circumstances, we have decided to optimize the geometry of HN_3 by the perfect-pairing multi-configuration (MC) SCF formalism[12] in which six frontier orbitals are invoked for six electrons (6,6) to be accommodated.[13] The CI energies calculated for this MC(6-6) SCF geometry[14] were found to be ca. 15 kJ mol^{-1} lower than those obtained for the RHF SCF optimized geometry.[14] The CI energies E_{CI} for the initial state $H+HN_3$ given in Table 1 are based on the above-mentioned MC SCF geometry for HN_3.

It should also be mentioned here that, in evaluating the CI energy of TS2, a series of CI computations were carried out at several points on the SCF reaction path to locate the point of the CI maximum. The geometry of TS2 given in Fig. 2 corresponds, in reality, to such a point where the N^1–N^2 linkage (1.89 Å) has considerably been elongated as compared to that in the SCF saddle point. It is now more than 100 kJ mol^{-1} less stable than the adduct radical **1**. The conclusion that TS2 is by far lower-lying than TS1 remains unaltered, however.

As can be seen in Table 1, the activation barrier heights for the rate-determining step (TS1) calculated by the MRD-CI/[4s2p1d] method, 18 (CI) and 21 (CI+vib) kJ mol^{-1}, are in good agreement with the experimental activation energy $E_a=19$ kJ mol^{-1}.[2] Also, the heat of reaction calculated for the overall process (1) by the same basis set, -324 kJ mol^{-1} (CI+vib), agrees well with the experimental value of $\Delta H_0^\circ=-320$ kJ mol^{-1}.[15]

Figure 3 is a diagrammatic illustration of the potential energy profiles for the $H+HN_3$ system calculated by the present MRD-CI/[4s2p1d]//6-31G(d,p) procedure. The energy gaps shown are all based on the CI energies with the vibrational zero-point energy corrections. That the reaction between H and HN_3 should end up with the formation of NH_2 ($^2B_1$)+N_2 via the rate-controlling TS1 is self-explanatory.

(C) Rate Constants. We are now in a position to calculate the bimolecular rate constants for

Table 1. Relative MRD-CI Energies (kJ mol^{-1}) of the H–HN_3 System Calculated by Use of the 6-31G(d,p) and [4s2p1d] Basis Functions

State	6-31G(d,p)			[4s2p1d]		Expt.
	UHF SCF	CI	CI+vib	CI	CI+vib	
H+HN_3	(0)[a]	(0)[b]	(0)[b]	(0)[c]	(0)[c]	(0)
TS1	50	27	30	18	21	19[d]
HHN_3(**1**)	−254	−347	−319	−393	−366	
$HHN_3(^2A')$	−243	−266	−242	−288	−264	
HN_3H(**2**)	−184	−13	12	−34	−9	
TS2	−240	−230	−219	−234	−222	
$NH_2(^2B_1)+N_2$	−437	−321	−309	−336	−324	−320[e]
$NH(^2A_1)+N_2$	−296	−182	−169	−194	−181	−198[f]
TS3	78	78	69	54	45	

a) $E_{SCF} = -164.34113$ hartrees. b) $E_{CI} = -164.86271$ hartrees; $E_{vib} = 54.8$ kJ mol^{-1}. c) $E_{CI} = -164.89389$ hartrees; $E_{vib} = 54.8$ kJ mol^{-1}. d) Experimental activation energy, E_a.[2] e) Based on the thermochemical data, ΔH_0°.[15] f) The excitation energy (123 kJ mol^{-1})[16] was corrected for the vibrational zero-point energy.

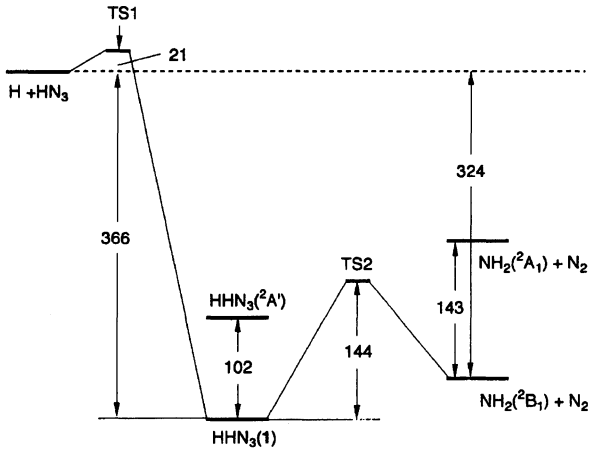

Fig. 3. Potential energy profiles of the H–HN_3 system calculated by the MRD-CI method employing the [4s2p1d] basis functions. Energy gaps shown are in units of kJ mol^{-1} with the vibrational zero point correction.

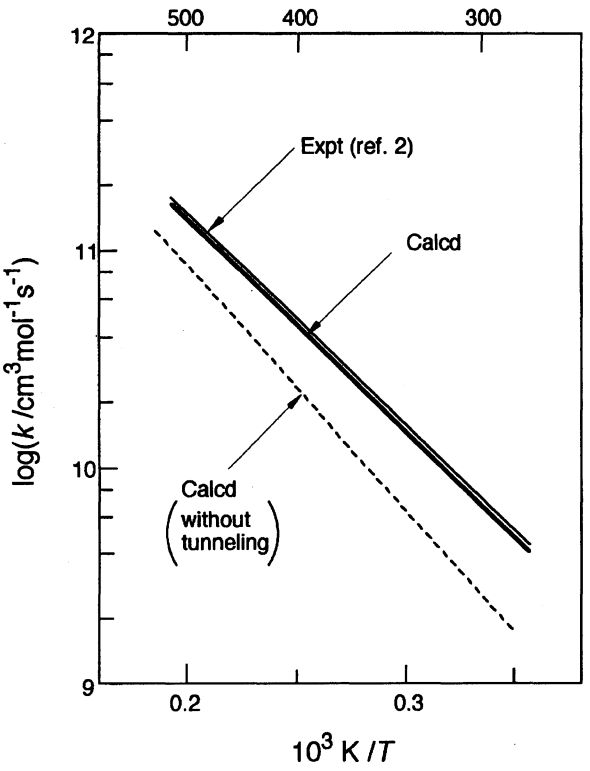

Fig. 4. Rate constants for the gas-phase reaction H+$HN_3 \rightarrow NH_2+H_2$. *Broken line*, calculated by the conventional TST without the tunneling correction; *bold line*, calculated by the TST formalism with the tunneling correction; *full line*, experimental results reported by G. Le Bras and J. Combourieu.[2]

reaction (1) according to the conventional transition state theory (TST). The vibrational frequencies calculated by the SCF/6-31G(d,p) procedure for the reactant HN_3 are 516.6, 609.3, 1130, 1292, 2260, and 3361 cm^{-1} (corrected by a constant factor of 0.90), which give the vibrational zero-point energy of 54.8 kJ mol^{-1}. The frequencies calculated by the same token for TS1 are 339.4, 454.0, 551.1, 635.2, 1058, 1286, 1942, and 3375 cm^{-1} with one additional imaginary frequency of $1256i$ cm^{-1}.

The rate constants k have first been calculated by adopting the [4s2p1d] theoretical activation energy E_0= 21 kJ mol^{-1} over the temperature range 300—500 K. The resuls are indicated by a dotted line in Fig. 4, where it is seen to be by a factor of 3 to 6 too low as compared with the experimental results,[2] which are represented by the Arrhenius parameters $A = 1.53 \times 10^{13}$ cm^3 mol^{-1} s^{-1} and E_a=19 kJ mol^{-1}. At first sight, the discrepancy may appear to be due to a possible overstimation of the E_0 value.

It is our feeling that another factor of importance which needs to be taken into consideration is the tunneling effect operative in the region of TS1. For evaluating the tunneling correction factors $\Gamma(T)$ at various

temperatures, we adopt here Wigner's expression[17]

$$\Gamma(T) = 1 + (h \mid \nu^{\ddagger} \mid /kT)^2/24, \quad (5)$$

where $\nu^{\ddagger}=1256i$ cm^{-1} in the present instance.

The $\Gamma(T)$ values at various temperatures were calculated according to Eq. 5. The rate constants k calculated by multiplying these $\Gamma(T)$ values at the temperature range 300—500 K are shown by a bold line in Fig. 4. The results reproduce the experimental curve quite satisfactorily. The theoretically obtained activation energy $E_0=21$ kJ mol^{-1} is believed to be highly accurate.

Discussion

As has already been described above, both the activation energy and the exoergicity of the entire reaction (1) are reproduced reasonably well by the present CI computations based on the [4s2p1d] basis functions. In view of this success, calculations of other energies related to the adduct radical (**1**) will also be sufficiently reliable. Thus, the H–N bond dissociation energy of **1** is calculated to be 366 kJ mol^{-1}, a value which is somewhat smaller than 440 kJ mol^{-1} for NH_3.[15] The energy barrier of **1** against its decomposition into NH_2+N_2 is predicted to be 144 kJ mol^{-1}. It seems, therefore, that the doublet radical **1** is a fairly stable entity and could well be identified as such when the H atom addition toward HN_3 is conducted under high pressures at low temperatures.

Also shown in Fig. 3 is the energy level for the planar ($^2A'$) form of HHN_3, which corresponds to the transition state for the "umbrella inversion" of HHN_3. The calculated inversion energy is 102 kJ mol^{-1}, which is significantly greater than the experimental value of 24 kJ mol^{-1} for the case of NH_3.[18]

At this stage, we would like to point out one feature of importance regarding the decomposition process (4). We have noticed that, as the N^1–N^2 bond of **1** is elongated, its NH_2 moiety is rotated increasingly around the N^1–N^2 axis until it attains a C_s-symmetric form at TS2. Beyond TS2, the entire system maintains the C_s symmetry all the way. An implication of this computational feature is that the NH_2 radical at the instance of its formation by the decomposition should be rotationally excited.

Finally, we will comment briefly on the abstraction reaction (2), which has been left out of account at the onset. Geometry optimization of the transition state (TS3) by the UHF/SCF procedure has given a structure as shown in Fig. 5. Results of the subsequent MRD-CI calculations are listed in the final line of Table 1. The activation energy (CI+vib) obtained by the use of the [4s2p1d] basis functions is 45 kJ mol^{-1}, which is clearly greater than that (21 kJ mol^{-1}) calculated for the addition reaction (1). Accordingly, the possibility of the abstraction reaction participating in the H–HN_3 reaction must be less than 0.5% in the temperature region of our interest. Ignoring the role of the abstraction reaction in the H–HN_3 reaction is thus most likely to be legitimate.

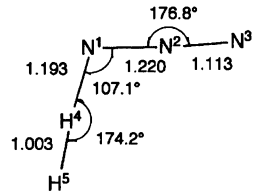

TS3 ($^2A'$)

Fig. 5. Optimized geometry of the transisiton state (TS3) for the abstraction reaction $H+HN_3 \rightarrow H_2+N_3$. The bond lengths are give in units of Å.

Conclusions

1. The gas-phase reaction $H+HN_3 \rightarrow NH_2+N_2$ should proceed through the rate-determining addition of H toward HN_3, the calculated barrier height being 21 kJ mol^{-1}.

2. The adduct radical HHN_3 could be a well-definable entity, which would, however, readily be collapsed into NH_2+N_2 above room temperature.

3. The conventional transition-state theory combined with tunneling corrections is capable of reproducing the bimolecular rate constants for the entire reaction in the temperature region 300—500 K.

This work was supported by the Grant-in-Aid for Scientific Research on Priority Areas No. 04243103 from the Ministry of Education, Science and Culture. The authors are grateful to Professor R. J. Buenker for supplying his Table MRD-CI program to them. All calculations were carried out on a HITAC M-680H at the Computer Center of the Institute for Molecular Science. The authors thank the Center for an allocation of CPU time.

References

1) O. Kajimoto, T. Yamamoto, and T. Fueno, *J. Phys. Chem.*, **83**, 429 (1979).

2) G. Le Bras and J. Combourieu, *Int. J. Chem. Kinet.*, **5**, 559 (1973).

3) S. Glastone, K. J. Laidler, and H. Eyring, "The Theory of Rate Processes," McGraw-Hill, New York (1941).

4) M. J. Frisch, J. S. Binkley, H. B. Schlegel, K. Raghavachari, C. F. Melius, R. L. Martin, J. J. P. Stewart, F. W. Bobrowicz, C. M. Rohlfing, L. R. Kahn, D. J. DeFrees, R. Seeger, R. A. Whiteside, D. J. Fox, E. M. Fleuder, S. Topiol, and J. A. Pople, "GAUSSIAN 86," Carnegie-Mellon Quantum Chemistry Publishing Unit, Pittsburgh (1984); IMS version registered by N. Koga, S. Yabushita, K. Sawabe, and K. Morokuma.

5) W. J. Hehre, R. Ditchfield, and J. A. Pople, *J. Chem. Phys.*, **56**, 2257 (1972); P. C. Hariharan and J. A. Pople,

Theor. Chim. Acta (*Berlin*), **28**, 213 (1973).

6) R. J. Buenker, "Studies in Physical and Theoretical Chemistry," ed by R. Carbo, Elsevier, Amsterdam, Vol. 21, pp. 17—34 (1982).

7) R. J. Buenker and R. A. Phillips, *J. Mol. Struct.* (*Theochem*), **123**, 291 (1985).

8) T. H. Dunning, Jr., *J. Chem. Phys.*, **53**, 2823 (1970).

9) T. Fueno, K. Yamaguchi, and O. Kondo, *Bull. Chem. Soc. Jpn.*, **63**, 901 (1990).

10) K. Yokoyama, S. Takane, and T. Fueno, *Bull. Chem. Soc. Jpn.*, **64**, 2230 (1991).

11) T. Fueno, K. Yokoyama, and S. Takane, *Theor. Chim. Acta* (*Berlin*), **82**, 299 (1992).

12) K. Morokuma, S. Kato, K. Kitaura, I. Ohmine, S. Sakai, and S. Obara, "IMSPAK," Institute for Molecular Science (1989).

13) The six orbitals in question are specifically the three highest occupied (8a′), (9a′), and (2a″) orbitals in conjunction with the three lowest vacant (10a′), (11a′), and (3a″) orbitals. The excited configuration which is mixed with the ground configuration most dominantly and to a not immaterial extent is the one that arises from the two-electron transition $(2a'')^2 \rightarrow (3a'')^2$.

14) The bond distances R (in Å) and angles θ (in degree) for HN_3 optimized by the MC(6-6) SCF procedure are as follows (the corresponding RHF results are given in parentheses): R (N^1–N^2)=1.250 (1.238), R (N^2–N^3)=1.123 (1.099), R (H^4–N^1)=1.005 (1.006), θ ($N^1N^2N^3$)=173.4° (173.8°), θ ($H^4N^1N^2$)=107.9° (108.2°).

15) S. W. Benson, "Thermochemical Kinetics," 2nd ed, Wiley, New York (1976).

16) G. Herzberg, "Electronic Spectra and Electronic Structure of Polyatomic Molecules," D. van Nostrand Co., New York (1966).

17) E. P. Wigner, *Z. Phys. Chem., Abt. B*, **19**, 203 (1932).

18) A. Rauk, L. C. Allen, and E. Clementi, *J. Chem. Phys.*, **52**, 4433 (1970).